OUKA
The University of Osaka
Institutional Knowledge Archive

Title	Benzo[cd]Perylenyl: A π-Expanded Phenalenyl Radical With Enhanced Aggregation Enthalpy and Stability
Author(s)	Ono, Yuga; Goto, Yuko; Tani, Yosuke et al.
Citation	Asian Journal of Organic Chemistry. 2025, p. e202500300
Version Type	VoR
URL	https://hdl.handle.net/11094/101399
rights	This article is licensed under a Creative Commons Attribution 4.0 International License.
Note	

The University of Osaka Institutional Knowledge Archive : OUKA

https://ir.library.osaka-u.ac.jp/

The University of Osaka

ACES Asian Chemical Editorial Society

doi.org/10.1002/ajoc.202500300

ASIAN JOURNAL OF ORGANIC CHEMISTRY
Research Article

www.asianjoc.org

Benzo[*cd*]Perylenyl: A π-Expanded Phenalenyl Radical With Enhanced Aggregation Enthalpy and Stability

Yuga Ono,[a] Yuko Goto,[a] Yosuke Tani,[a] Kazuhiro Nakasuji,[a] Kazunobu Sato,[b] Takeji Takui,[b] Daiki Shimizu,[c] Kenji Matsuda,[c] and Takashi Kubo*[a, d, e]

Dedicated to the memory of Professor Masahiko Iyoda

We report the synthesis and characterization of a π-expanded neutral PAH radical, benzo[*cd*]perylenyl (**1**) derived from the phenalenyl radical (**2**). Hückel molecular orbital (HMO) analysis reveals a uniformly distributed SOMO that enables effective two-electron 20-center bonding in a π-dimer. ESR measurements of **1** show a long half-life of 63 days in air-saturated toluene at room temperature. Temperature-dependent ESR and absorption spectra as well as DFT calculations confirm the preferential formation of a π-dimer over a σ-dimer with an association energy of approximately -65 kJ mol^{-1}, driven by enhanced dispersion interactions. These findings demonstrate that π-expansion stabilizes organic radicals without bulky substituents while preserving intermolecular interactions offering new prospects for advanced materials in electronics and spintronics.

1. Introduction

Organic π-conjugated radical species have attracted significant attention due to their unique electronic spin properties, making them widely studied as materials for electronics and spintronics applications.[1–4] In recent years, there has been growing interest in the luminescent properties of such radicals with potential applications in organic electroluminescent (EL) devices and sensors being actively explored.[5] However, radicals by their very nature contain unpaired electrons making them highly reactive. They tend to undergo rapid deactivation through reactions such as oxygen addition, hydrogen atom abstraction, or the formation of σ-bonded dimers (commonly referred to as σ-dimers). Consequently, conventional approaches to obtaining long-lived or stable radical species have primarily relied on introducing bulky substituents to physically hinder intermolecular contact.[6] While this strategy effectively stabilizes radicals, it also suppresses intermolecular interactions making it difficult to achieve the unique physical properties and functionalities arising from unpaired electron interactions between molecules.

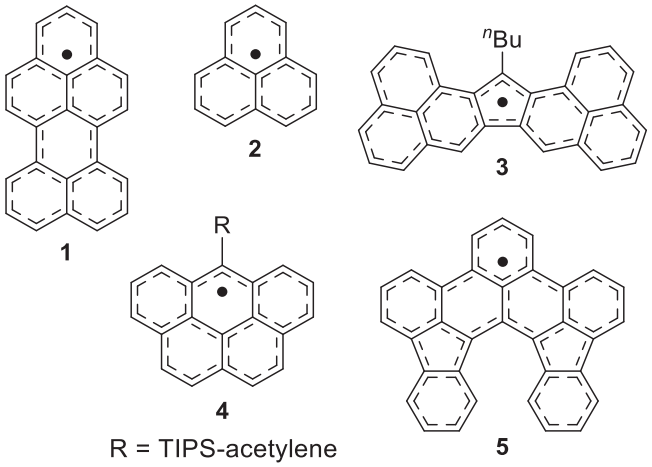

Scheme 1. Sterically unhindered PAH radicals.

Alternatively, expanding the π-conjugation can enhance the delocalization of an unpaired electron, contributing to the stabilization of radical species. Among hydrocarbon radicals, compounds (**3**, **4**, **5**) with highly delocalized unpaired electrons exhibit sufficiently long lifetimes allowing them to be handled under ambient conditions without special precautions (Scheme 1).[7–9] Such organic radical species, which possess an expanded π-conjugated system but lack bulky steric

[a] Y. Ono, Y. Goto, Dr. Y. Tani, Prof. Dr. K. Nakasuji, Prof. Dr. T. Kubo
Department of Chemistry, Graduate School of Science, The University of Osaka, Toyonaka, Osaka 560-0043, Japan
E-mail: kubo@chem.sci.osaka-u.ac.jp

[b] Prof. Dr. K. Sato, Prof. Dr. T. Takui
Department of Chemistry, Graduate School of Science, Osaka Metropolitan University, Sumiyoshi-ku, Osaka 558-8585, Japan

[c] Dr. D. Shimizu, Prof. Dr. K. Matsuda
Department of Synthetic Chemistry and Biological Chemistry, Graduate School of Engineering, Kyoto University, Nishikyo-ku, Kyoto 615-8510, Japan

[d] Prof. Dr. T. Kubo
Innovative Catalysis Science Division, Institute for Open and Transdisciplinary Research Initiatives (ICS-OTRI), The University of Osaka, Suita, Osaka 565-0871, Japan

[e] Prof. Dr. T. Kubo
Spintronics Research Network Division, Institute for Open and Transdisciplinary Research Initiatives (SPIN-OTRI), The University of Osaka, Suita, Osaka 565-0871, Japan

Supporting information for this article is available on the WWW under https://doi.org/10.1002/ajoc.202500300

© 2025 The Author(s). Asian Journal of Organic Chemistry published by Wiley-VCH GmbH. This is an open access article under the terms of the Creative Commons Attribution License, which permits use, distribution and reproduction in any medium, provided the original work is properly cited.

© 2025 The Author(s). Asian Journal of Organic Chemistry published by Wiley-VCH GmbH

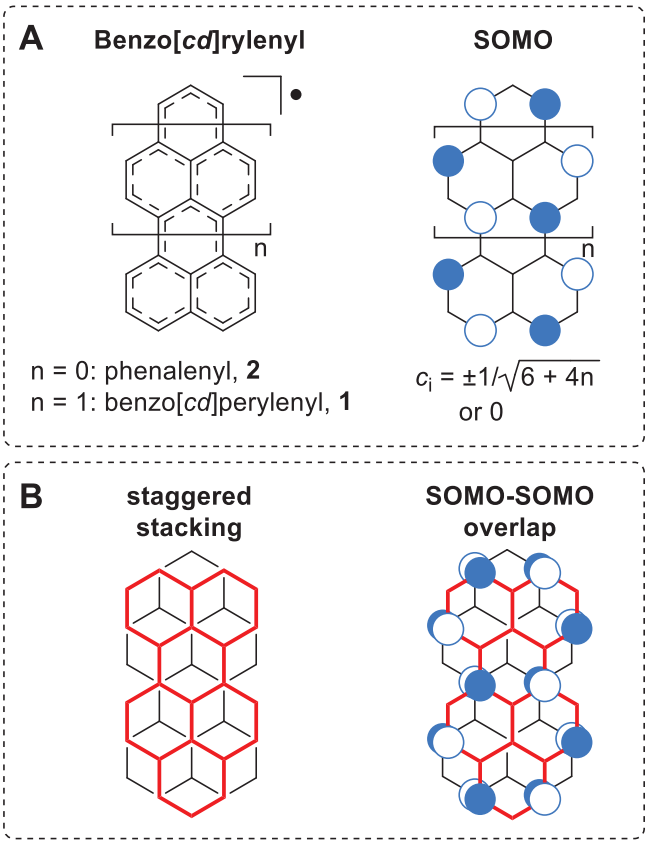

Figure 1. (A) Chemical structure and SOMO (c_i, the coefficients of SOMO under the HMO theory) of benzo[*cd*]rylenyl. (B) Staggered stacking of **1** and it's SOMO–SOMO overlap.

protection groups tend to form dimeric aggregates (namely, π-dimers) through $\pi-\pi$ stacking interactions. A key feature of π-dimers is the formation of two-electron multicenter (2e/mc) bonding between the two unpaired electrons.[10–19] This bonding mode, where multiple atoms share a single electron pair not only expands conventional bonding concepts and electronic structure models but also holds promise for breakthroughs in functional design, enabling precise control over spin, charge transport, nonlinear optical properties, and luminescence characteristics.

In this study, we report the synthesis of a neutral PAH radical, benzo[*cd*]perylenyl (**1**), which is π-expanded from the phenalenyl radical (**2**), and the investigation of its fundamental electronic structure and π-dimerization behavior.

2. Results and Discussion

2.1. Electronic Structure of Benzo[*cd*]Ryleneyl

The title compound **1** is the smallest odd-alternant hydrocarbon within the benzo[*cd*]rylenyl family (Figure 1A). According to Ovchinnikov's rule, benzo[*cd*]rylenyl inherently adopts a mono radical character (that is, $S = 1/2$) due to the difference of one between the number of starred and unstarred carbon atoms. Within the framework of Hückel molecular orbital (HMO) theory, the singly-occupied molecular orbital (SOMO) extends across the entire molecule but remains localized exclusively on the starred carbon atoms, with an equal amplitude of $c_i = \pm 1/\sqrt{6+4n}$. This uniform distribution of the SOMO is a defining feature of the electronic structure of benzo[*cd*]rylenyl and plays a pivotal role in its π-stacking behavior. Notably, even in a staggered stacking arrangement designed to minimize interatomic repulsion, the SOMOs of adjacent molecules exhibit perfect overlap (Figure 1B). This extensive orbital interaction enhances the coupling between unpaired electrons (that is, two-electron 20-center (2e/20c) bonding), thereby facilitating efficient spin and charge transport within an infinite π-stacking system.

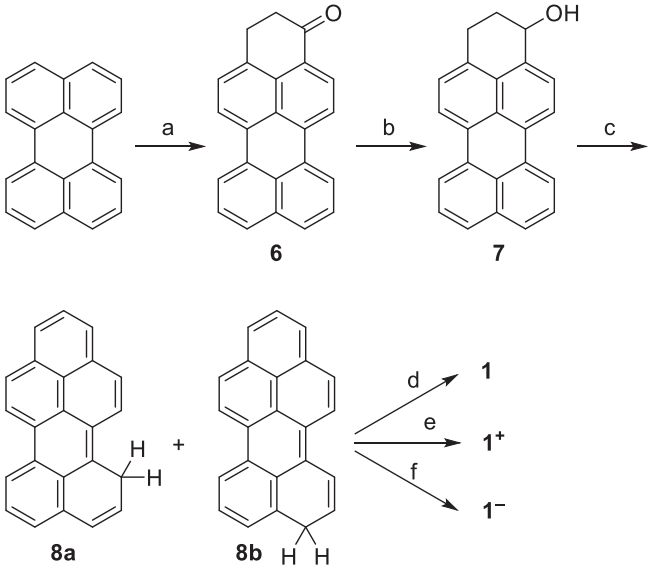

Scheme 2. Synthetic route for **1**, 1^+, and 1^-. (A) Acrylic acid, $(CF_3CO)_2O$, CF_3SO_3H, 0 °C, 25% yield; (B) $NaBH_4$, CH_2Cl_2, CH_3OH, RT, 85%; (C) *p*-TsOH·H_2O (cat.), toluene, reflux, 95%; (D) *p*-chloranil, toluene, 60 °C, 86%; (e) $Ph_3C^+ \cdot BF_4^-$, CH_2Cl_2, RT, 57%; (f) *n*-BuLi, THF-d_8 in a sealed degassed tube.

2.2. Synthesis and Characterization of 1

The precursor (**8a**, **8b**) of the radical **1** was synthesized by a procedure (Scheme 2) modified from the method developed by Yamamura and Murata.[20] According to the report by Plażuk et al.,[21] we could obtain a cyclic ketone **6** directly from perylene. The reduction of **6** with $NaBH_4$ gave rise to alcohol **7**. The dehydration of **7** with *p*-toluenesulfonic acid (*p*-TsOH) yielded a mixture of two isomerized hydro-precursors, **8a** and **8b**. The structure of **8a** and **8b** was determined by a ^{1}H NMR spectroscopy and density functional theory (DFT) calculations (see Table S1 and Figure S1). The target radical **1** was obtained as a dark green microcrystalline powder by treatment of **8a** and **8b** with *p*-chloranil. In addition, corresponding cation 1^+ and anion 1^- species were also generated by treating **8a** and **8b** with triphenylmethyl tetrafluoroborate and *n*-butyllithium, respectively.

A toluene solution of **1** exhibited a well-resolved multiline ESR spectrum at room temperature. However, the complexity of the pattern posed challenges in accurately determining the

© 2025 The Author(s). Asian Journal of Organic Chemistry published by Wiley-VCH GmbH

21935815, 0, Downloaded from https://aces.onlinelibrary.wiley.com/doi/10.1002/ajoc.202500300 by The University Of Osaka, Wiley Online Library on [01/05/2025]. See the Terms and Conditions (https://onlinelibrary.wiley.com/terms-and-conditions) on Wiley Online Library for rules of use; OA articles are governed by the applicable Creative Commons License

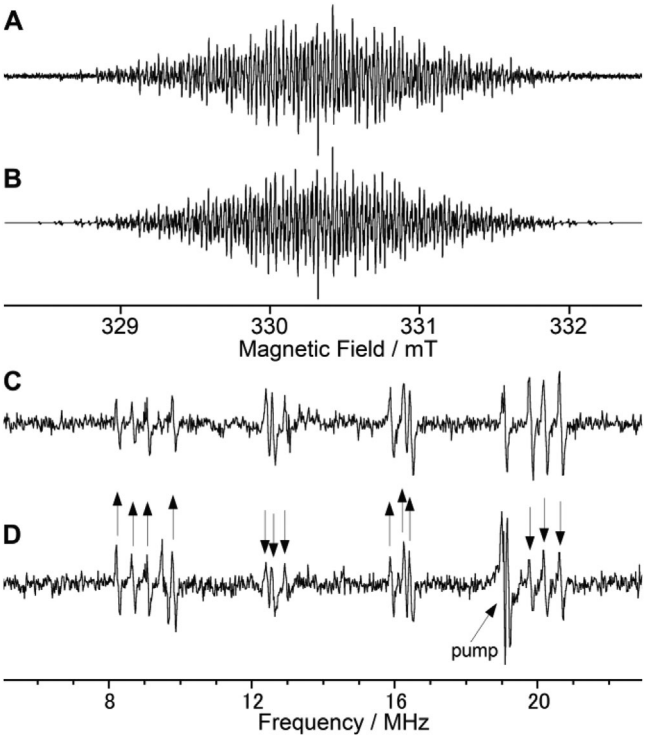

Figure 2. (A) Observed ESR spectrum of **1** in toluene (1×10^{-4} M) at room temperature. The g value was determined experimentally to be 2.0027. (B) Corresponding simulated spectrum. (C) ^{1}H ENDOR and (D) TRIPLE (pump frequency, 19.1 MHz) spectra recorded at 240 K for **1** in toluene (5×10^{-4} M). The vertical upward and downward arrows denote the increase and decease in ENDOR intensity at the resonance frequency during the pumping in TRIPLE spectroscopy. The hyperfine coupling constants (a_H) determined by ENDOR/TRIPLE experiments are −12.4, −11.5, −10.7, −9.24, +3.96, +3.66, and +2.93 MHz, which correspond to −0.442, −0.410, −0.381, −0.328, +0.141, +0.130, and + 0.104 mT, respectively.

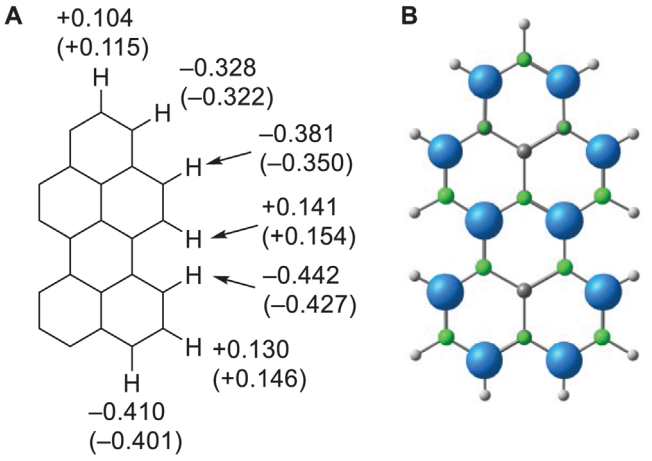

Figure 3. (A) The assignment of a^H values. In parenthesis, the a_H values calculated with a UBLYP/6–31G**//UB3LYP/6–31G** method and the McConnell model ($Q = -2.4$ mT).[22] (B) Spin density map calculated with a UBLYP/6–31G**//UB3LYP-D3/6–31G** method. Blue and green surfaces represent α and β spin densities drawn at 0.004 e/au^3 level, respectively.

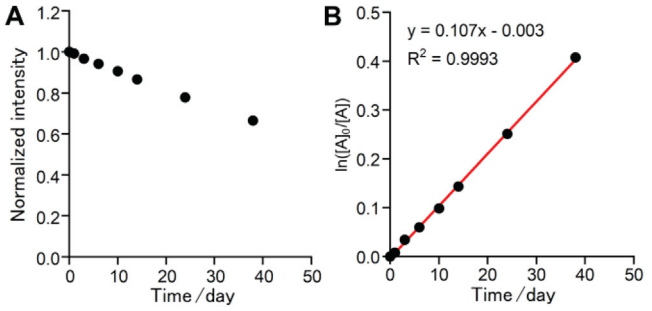

Figure 4. (A) Normalized intensities of time dependent ESR (initial concentration is 1×10^{-4} M in air-saturated toluene, room temperature, under dark condition) measurement of **1**. (B) The approximate correspondence with first order kinetic equation.

proton hyperfine coupling constants (a_H) through computer simulation. To obtain the most reliable a_H values, we employed the ENDOR/TRIPLE technique, which provides both the magnitudes and relative signs of the hyperfine couplings. Figure 2 shows the experimentally observed ESR spectrum of **1** alongside the simulated spectrum, and the corresponding ^{1}H ENDOR/TRIPLE spectra are also shown. The excellent agreement between the experimental and theoretical a_H values (Figure 3A) suggests that the unpaired electron delocalizes over the whole of the molecule.

The stability of **1** was evaluated by monitoring the decay of its ESR signal intensity in an air-saturated toluene solution at room temperature under dark conditions (Figure 4). Notably, **1** exhibits a half-life of 63 days, which is exceptionally long when compared to the phenalenyl radical **2**, which undergoes rapid oxidation in the presence of oxygen.[23] This remarkable stability of **1** is primarily attributed to π-expansion because other π-expanded PAH radicals, **3**, **4**, and **5**, also demonstrate long half-lives of 60 h,[7] 7 days,[8] and over 62 h,[9] respectively. The long-lasting nature of **1** would be related to its thermodynamic stability higher than that of **2**. The thermodynamic stability of neutral radicals can be assessed using radical stabilization energy (RSE),[24] which is determined through 2nd-order restricted open-shell Møller–Plesset perturbation theory (ROMP2) calculations for isodesmic hydrogen transfer reactions. We computed the RSE values for **1** and **2** at the ROMP2/6–31G**//UB3LYP-D3/6–31G** level of theory. The calculated RSE values (in kJ mol^{-1}) were −214.4 for **1** and −201.6 for **2**, indicating the exceptionally high thermodynamic stability of **1**.

The cyclic voltammogram of **1** in CH_2Cl_2 revealed two reversible redox waves: the half-wave potentials for oxidation ($E_{ox}^{1/2}$) and reduction waves ($E_{red}^{1/2}$) are −0.22 V and −1.42 V vs Fc/Fc$^+$, respectively (Figure 5). The potential difference between the oxidation and reduction waves is 1.20 V, corresponding to the disproportionation potential (ΔE) of **1**. Notably, this ΔE value is significantly smaller than that of **2** (1.6 V), supporting that **1** possesses greater thermodynamic stability due to wider spin delocalization.[25] To investigate the electronic structure of the oxidized and reduced species of **1**, we generated cation (**1**$^+$) and anion (**1**$^-$) species by the reaction of the hydro-precursors **8a** and **8b** with triphenylmethyl cation and *n*-butyllithium, respectively. ^{1}H and ^{13}C NMR chemical shifts are shown in Figure S2. The total ^{13}C chemical shift change ($\Sigma\Delta\delta_C$) of the sp^2 carbon atoms on going from **1**$^+$ to **1**$^-$ is 293.64 ppm (or 146.82 per electron),

© 2025 The Author(s). Asian Journal of Organic Chemistry published by Wiley-VCH GmbH

21935815, 0, Downloaded from https://aces.onlinelibrary.wiley.com/doi/10.1002/ajoc.202500300 by The University Of Osaka, Wiley Online Library on [01/05/2025]. See the Terms and Conditions (https://onlinelibrary.wiley.com/terms-and-conditions) on Wiley Online Library for rules of use; OA articles are governed by the applicable Creative Commons License

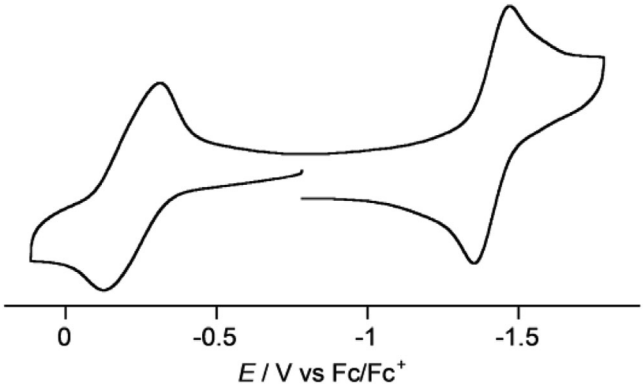

Figure 5. Cyclic voltammogram of **1** in CH_2Cl_2 (1.0×10^{-3} M) with 0.1 M $^nBu_4NPF_6$ as the supporting electrolyte at room temperature. Sweep rate = 0.1 V s^{-1}. The slightly broader oxidation wave compared to the reduction wave may be due to partial dimerization between the cationic species and the neutral radical species.

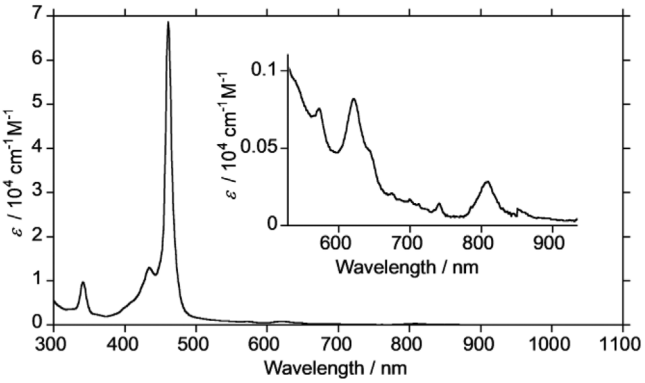

Figure 6. Electronic absorption spectrum (1×10^{-4} M in toluene, room temperature) of **1**. Inset shows a magnified view in the long wavelength region.

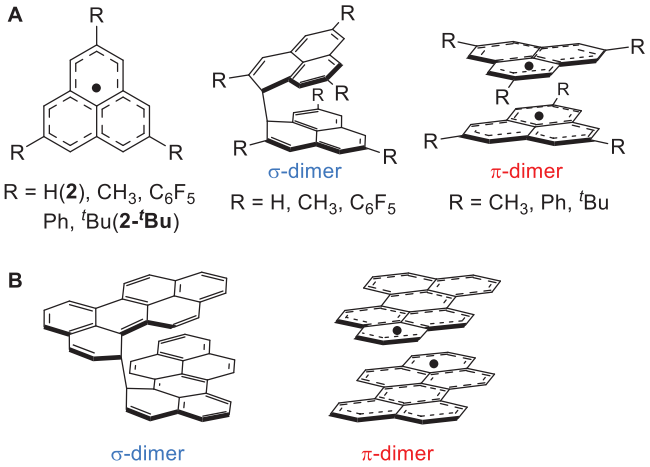

Scheme 3. Dimerization mode of ([A] phenalenyl radicals and (B) benzo[*cd*]perylenyl **1**.

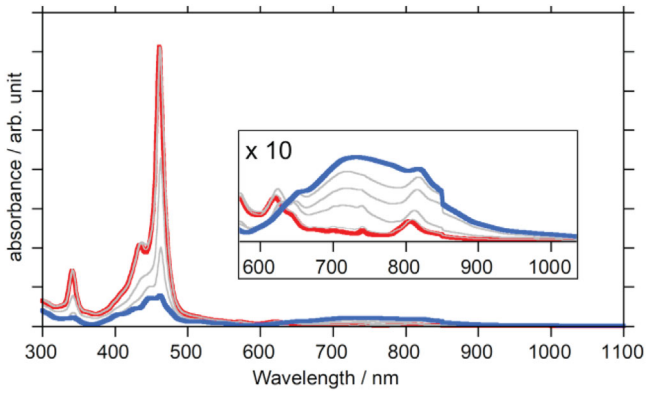

Figure 7. Variable temperature electronic absorption spectra (1×10^{-4} M in toluene) of **1**. Inset shows a magnified view in the long wavelength region. Temperature from red to bule (K): 300, 280, 260, 240, 220, 200.

which is in good agreement with the Spiesecke and Schneider correlation predicting a total ^{13}C chemical shift of 160 ppm per unit charge.[26] The shift changes are large for the carbon atoms with $c_i = \pm 1/\sqrt{10}$ but small for the other carbons (Figure S3). This finding indicates that SOMO is actually involved in the redox process.

Figure 6 shows the electronic absorption spectrum of **1** measured in toluene at room temperature. The spectrum features a weak long-wavelength absorption band at 807 nm ($\varepsilon = 300$ cm^{-1} M^{-1}) and a strongly intense short-wavelength band at 459 nm ($\varepsilon = 68600$). This spectral pattern is similar to that of the tri-*tert*-butyl derivative of **2** (**2-^{t}Bu**, see Scheme 3), which exhibits a forbidden transition at 544 nm ($\varepsilon = 103$) and an allowed transition at 342 nm ($\varepsilon = 26700$), as shown in Figure S4.[27] However, the bands of **1** are red-shifted compared to those of **2-^{t}Bu**. Time-dependent (TD) DFT calculations (UB3LYP/6–31G**) of **1** revealed that the weak absorption at 807 nm and the intense absorption at 459 nm correspond to in-phase and out-of-phase interactions, respectively, of the two excited configurations arising from excitation of an electron into and out of SOMO (Figure S5).

2.3. Association Behavior of 1

Temperature modulation of the electronic absorption spectrum of **1** revealed a notable increase in the intensity of the 720 nm absorption band with decreasing temperature (Figure 7). Similar behavior was observed for **2-^{t}Bu**, which exhibits the growth of the 595 nm band upon cooling, attributed to π-dimer formation.[28] Accordingly, the low-energy absorptin band of **1** is likely associated with the formation of a π-dimer. However, as previously noted, organic radicals can form either σ-dimers or π-dimers, as exemplified by the dimerization behavior of **2** derivatives (Scheme 3).[29,30] To assess the relative stability of these dimeric forms, we estimated the association energies (ΔE_D) of **1** for σ- and π-dimerizations using DFT calculations with M05-2X/6–31G** method, which has been shown by Kertesz et al. to best reproduce the π-dimerization energy of phenalenyl radicals.[15] The calculated values were ΔE_D (σ-dimer) = −30 kJ mol^{-1} and ΔE_D (π-dimer) = −65 kJ mol^{-1}, indicating a significantly stronger stabilization for the π-dimer (see also Figure S6—S7, Table S2 for ΔE_D of other σ- and π-dimers). This substantial energy difference strongly suggests that **1** preferentially forms a π-dimer at low temperatures. Indeed, TD-B3LYP/6–31G**

© 2025 The Author(s). Asian Journal of Organic Chemistry published by Wiley-VCH GmbH

21935815, 0, Downloaded from https://aces.onlinelibrary.wiley.com/doi/10.1002/ajoc.202500300 by The University Of Osaka, Wiley Online Library on [01/05/2025]. See the Terms and Conditions (https://onlinelibrary.wiley.com/terms-and-conditions) on Wiley Online Library for rules of use; OA articles are governed by the applicable Creative Commons License

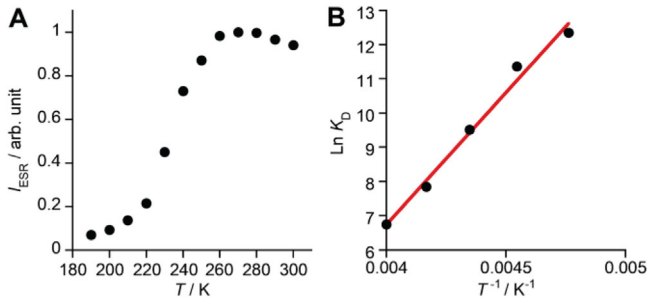

Figure 8. Temperature dependence of (A) ESR signal intensity (I_{ESR}) and (B) the dimerization constant (K_D) of **1**. The ESR signal intensities at each temperature were determined by double integral of the signals with the use of Mn^{2+} standard for normalization.

Table 1. Thermodynamic parameters (ΔH_D in kJ mol^{-1} and ΔS_D in eu) for π-dimerization of radicals, selected intermolecular interaction energy (ΔE in kJ mol^{-1}) in π-dimers based on the ALMO-EDA analysis, and singlet–triplet energy gap (ΔE_{S-T} in kJ mol^{-1}) of π-dimers.

	VT-ESR		ALMO-EDA[C]			DFT
	ΔH_D	ΔS_D	ΔE_{total}	ΔE_{ct}	ΔE_{disp}	ΔE_{S-T}
1[A]	−64	−201	−43	−62	−158	−57
2[A]	n.d.	n.d.	−27	−47	−95	−60
2-^{t}Bu[B]	−40	−150	−39	−25	−96	−31

[A] The structure of π-dimer used in the ALMO-EDA analysis was obtained by the broken symmetry UM05-2X/6–31G** calculation method. [B] The structure of π-dimer used in the ALMO-EDA analysis was obtained from X-ray crystallographic analysis. [C] See Table S3 for all the interaction energies.

calculations predict that a π-dimer of **1** shows a low-energy absorption band at 706 nm ($f = 0.266$), which corresponds to a HOMO→LUMO transition in the π-dimer further supporting this assignment.

The ESR signal intensity of **1** progressively decreased with decreasing temperature and nearly vanished at 190 K (Figure 8). This reduction in signal intensity is attributed to the formation of a diamagnetic π-dimer. The variable-temperature ESR measurements allowed us to determine the thermodynamic parameters for the dimerization process, yielding an enthalpy change (ΔH_D) of −64 kJ mol^{-1} and an entropy change (ΔS_D) of − 201 eu. The ΔH_D is in good agreement with the theoretically estimated association energy ($\Delta E_D = -65$ kJ mol^{-1}).

The ΔH_D for the π-dimerization of **1** is significantly larger than that of the phenalenyl radical (**2-^{t}Bu**), as summarized in Table 1. This enhanced stabilization is likely due to the larger π-plane of **1**, which facilitates stronger $\pi-\pi$ interactions between molecules, as well as due to the perfect SOMO–SOMO overlap (that is, two-electron 20-center (2e/20c) bonding). For the quantitative argument, we employed the absolutely localized molecular orbital energy decomposition analysis (ALMO–EDA), which is a quantum mechanical treatment for analyzing intermolecular interactions. As shown in Table 1, the intermolecular interactions in the π-dimers of **1** and **2** show a significant difference in dispersion energy (ΔE_{disp}). This is because the π-plane of **1** is considerably larger than that of **2**. In fact, **1** has a larger ΔE_{disp} than the phenalenyl radical with *tert*-butyl groups (**2-^{t}Bu**), which are known to exhibit strong dispersion interactions. This indicates that a $\pi-\pi$ interaction plays a crucial role in the strong association nature of **1**.

On the other hand, the charge-transfer energy (ΔE_{ct}), which reflects orbital interactions, is only slightly larger in **1** compared to **2**. Because both π-dimers are composed of neutral identical species, this small difference in the ΔE_{ct} values is in line with that the SOMO–SOMO overlap in both π-dimers is nearly perfect. Furthermore, the energy gap between singlet and triplet state (ΔE_{S-T}), which is estimated by the DFT calculations, is almost the same for the two π-dimers. This consistency with the similarity in ΔE_{ct} between **1** and **2** suggests that the covalent bonding interaction between the two unpaired electrons in both π-dimers is nearly identical.

3. Conclusion

This study demonstrated that π-expansion can effectively stabilize organic radicals without relying on bulky substituents. Our investigation of benzo[*cd*]perylenyl (**1**) revealed that its widely delocalized SOMO not only underpins remarkable intrinsic stability but also drives the formation of π-dimers through optimal SOMO–SOMO overlap. Combined experimental and computational studies indicated that the stabilization of **1** arises from favorable thermodynamic factors, while dispersion interactions play a crucial role in governing π-dimer formation. These insights open new avenues for designing organic materials with tailored spin and charge transport properties and lay the groundwork for further exploration of π-expanded systems in electronic and spintronic applications.

Acknowledgements

T.K. thanks the JSPS for KAKENHI funding (Grant No. JP24H00459) and a Grant-in-Aid for Transformative Research Areas (A) "Condensed Conjugation" (JSPS for KAKENHI funding Grant No. JP20H05865) from MEXT, Japan. T.Y. thanks the JSPS for KAKENHI funding (JP23K23427, JP23H03955). D.S. thanks the JSPS for KAKENHI funding (JP20H05866, JP20H05868). Theoretical calculations were performed at the Research Center for Computational Science, Okazaki, Japan. The EDA calculations were conducted on the Super Computer System, Institute for Chemical Research, Kyoto University.

Conflict of Interests

The authors declare no conflict of interest.

Data Availability Statement

The data that support the findings of this study are available in the supplementary material of this article.

© 2025 The Author(s). Asian Journal of Organic Chemistry published by Wiley-VCH GmbH

21935815, 0, Downloaded from https://aces.onlinelibrary.wiley.com/doi/10.1002/ajoc.202500300 by The University Of Osaka, Wiley Online Library on [01/05/2025]. See the Terms and Conditions (https://onlinelibrary.wiley.com/terms-and-conditions) on Wiley Online Library for rules of use; OA articles are governed by the applicable Creative Commons License

Keywords: Neutral radical · Phenalenyl radical · Polycyclic aromatic hydrocarbon · Two electron multicenter bonding · Π-dimer

[1] Z. X. Chen, Y. Li, F. Huang, *Chem* **2021**, *7*, 288–332.
[2] L. Ji, J. Shi, J. Wei, T. Yu, W. Huang, *Adv. Mater.* **2020**, *32*, 1908015.
[3] T. Kubo, M. Abe, *Chem. Rev.* **2024**, *124*, 4541–4542.
[4] J. Xu, S. Li, Y. Yang, Z. Chen, *Chem. - Eur. J.* **2023**, *29*, e202203598.
[5] A. Mizuno, R. Matsuoka, T. Mibu, T. Kusamoto, *Chem. Rev.* **2024**, *124*, 1034–1121.
[6] D. Griller, K. U. Ingold, *Acc. Chem. Res.* **1976**, *9*, 13–19.
[7] T. Kubo, Y. Katada, A. Shimizu, Y. Hirao, K. Sato, T. Takui, M. Uruichi, K. Yakushi, R. C. Haddon, *J. Am. Chem. Soc.* **2011**, *133*, 14240–14243.
[8] Q. Xiang, J. Guo, J. Xu, S. Ding, Z. Li, G. Li, H. Phan, Y. Gu, Y. Dang, Z. Xu, Z. Gong, W. Hu, Z. Zeng, J. Wu, Z. Sun, *J. Am. Chem. Soc.* **2020**, *142*, 11022–11031.
[9] H. Hamamoto, D. Shimizu, K. Matsuda, *Chem. - Eur. J.* **2024**, *30*, e202401353.
[10] J. J. Novoa, P. Lafuente, R. E. Del Sesto, J. S. Miller, *Angew. Chem., Int. Ed.* **2001**, *40*, 2540–2545.
[11] J. S. Miller, J. J. Novoa, *Acc. Chem. Res.* **2007**, *40*, 189–196.
[12] F. Mota, J. S. Miller, J. J. Novoa, *J. Am. Chem. Soc.* **2009**, *131*, 7699–7707.
[13] Z. Cui, H. Lischka, H. Z. Beneberu, M. Kertesz, *J. Am. Chem. Soc.* **2014**, *136*, 12958–12965.
[14] Z. Cui, H. Lischka, T. Mueller, F. Plasser, M. Kertesz, *ChemPhysChem* **2014**, *15*, 165–176.
[15] Z. Mou, Y.-H. Tian, M. Kertesz, *Phys. Chem. Chem. Phys.* **2017**, *19*, 24761–24768.
[16] Z. Mou, M. Kertesz, *Angew. Chem., Int. Ed.* **2017**, *56*, 10188–10191.
[17] M. Kertesz, *Chem. - Eur. J.* **2019**, *25*, 400–416.
[18] Z. Cui, M. Wang, H. Lischka, M. Kertesz, *JACS Au* **2021**, *1*, 1647–1655.
[19] K. E. Preuss, *Polyhedron* **2014**, *79*, 1–15.
[20] K. Yamamura, H. Miyake, I. Murata, *J. Org. Chem.* **1986**, *51*, 251–253.
[21] M. Głodek, A. Makal, A. Kłys, J. Zakrzewski, D. Plażuk, *Eur. J. Org. Chem.* **2016**, *2016*, 4215–4223.
[22] H. M. McConnell, *J. Chem. Phys.* **1956**, *24*, 764–766.
[23] D. H. Reid, *Tetrahedron* **1958**, *3*, 339–352.
[24] J. Hioe, H. Zipse, *Org. Biomol. Chem.* **2010**, *8*, 3609–3617.
[25] O. A. Levitskiy, V. V. Sentyurin, A. V. Bogdanov, T. V. Magdesieva, *Electrochim. Acta* **2023**, *460*, 142632.
[26] H. Spiesecke, W. G. Schneider, *Tetrahedron Lett.* **1961**, *2*, 468–472.
[27] K. Goto, T. Kubo, K. Yamamoto, K. Nakasuji, K. Sato, D. Shiomi, T. Takui, M. Kubota, T. Kobayashi, K. Yakusi, J. Ouyang, *J. Am. Chem. Soc.* **1999**, *121*, 1619–1620.
[28] D. Small, V. Zaitsev, Y. Jung, S. V. Rosokha, M. Head-Gordon, J. K. Kochi, *J. Am. Chem. Soc.* **2004**, *126*, 13850–13858.
[29] Z. Mou, K. Uchida, T. Kubo, M. Kertesz, *J. Am. Chem. Soc.* **2014**, *136*, 18009–18022.
[30] K. Uchida, Z. Mou, M. Kertesz, T. Kubo, *J. Am. Chem. Soc.* **2016**, *138*, 4665–4672.

Manuscript received: March 7, 2025
Revised manuscript received: March 27, 2025
Version of record online: ■■, ■■

© 2025 The Author(s). Asian Journal of Organic Chemistry published by Wiley-VCH GmbH

21935815, 0, Downloaded from https://aces.onlinelibrary.wiley.com/doi/10.1002/ajoc.202500300 by The University Of Osaka, Wiley Online Library on [01/05/2025]. See the Terms and Conditions (https://onlinelibrary.wiley.com/terms-and-conditions) on Wiley Online Library for rules of use; OA articles are governed by the applicable Creative Commons License